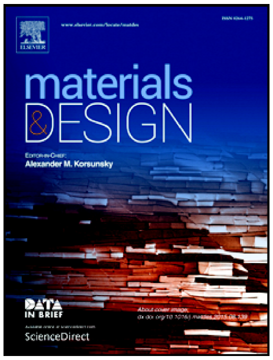

Non-volatile, Li-doped ion gel electrolytes for flexible WO3-based electrochromic devices

Tae Yong Yun, Xinlin Li, Jaehyun Bae, Se Hyun Kim, Hong Chul Moon

PII: S0264-1275(18)30822-0
DOI: https://doi.org/10.1016/j.matdes.2018.11.016
Reference: JMADE 7481

To appear in: *Materials & Design*

Received date: 13 July 2018
Revised date: 5 November 2018
Accepted date: 7 November 2018

Please cite this article as: Tae Yong Yun, Xinlin Li, Jaehyun Bae, Se Hyun Kim, Hong Chul Moon , Non-volatile, Li-doped ion gel electrolytes for flexible WO3-based electrochromic devices. Jmade (2018), https://doi.org/10.1016/j.matdes.2018.11.016

Non-Volatile, Li-Doped Ion Gel Electrolytes for Flexible WO_3-Based Electrochromic Devices

Tae Yong Yun[1,†] *Xinlin Li*[2,†], *Jaehyun Bae*[3], *Se Hyun Kim*,[2,3]* *and Hong Chul Moon*,[1]*

[1]Department of Chemical Engineering, University of Seoul, Seoul 02504, Republic of Korea
[2]Department of Mechanical Engineering Science, Yeungnam University, Gyeongsan, North Gyeongsang 38541, Republic of Korea
[3]School of Chemical Engineering, Yeungnam University, Gyeongsan, North Gyeongsang 38541, Republic of Korea

*Corresponding authors: hcmoon@uos.ac.kr, shkim97@yu.ac.kr

[†]These authors equally contributed to this work.

Abstract

Flexible electrochromic devices (ECDs) based on Li-doped ion gels and tungsten trioxide (WO_3) are demonstrated. Colored ECDs cannot be produced using conventional ion gels comprised of copolymers and room temperature ionic liquids (RTILs) due to a lack of cations that can be inserted into WO_3. Based on considerations of the coloration mechanism, we developed Li-doped ion gels and applied these to devices. The effects of Li salt concentration are systematically examined, with respect to device dynamics, coloration efficiency, and transmittance contrast. In addition, the coloration/bleaching switching stability of the ECD produced using optimal Li salt content is investigated. The ECD exhibits distinct colored and bleached states even after 24 h operation in air. Using the described Li-doped ion gel electrolytes, flexible WO_3 ECDs were successfully demonstrated with good bending stability and no electrolyte leakage.

Keywords: Li-doped gels, Electrochromism, Flexible Device, Tungsten Oxide

1. Introduction

Electrochemical devices have been utilized in diverse applications including batteries [1-5], supercapacitors [6-11], sensors [11-13], and actuators [14-16]. In particular, the development of electrochemical displays such as electrochemiluminescence devices has attracted great attention due to their simplicity [17-21]. Electrochromic devices (ECDs) capable of changing optical properties (e.g. absorbance and transmittance) according to an applied voltage are representative of electrochemical displays [22-47]. Traditional ECD uses include anti-glare mirrors, smart glasses, and displays. However, new applications have been identified recently, for example, electronic skins (e-skins) [42-44], and electrochromic supercapacitors (ECSs) [45-47]. Also, the realization of flexible/stretchable devices is viewed as a challenge for future wearable electronics.

Inorganic electrochromic materials are preferred to organic materials, because of their better photochemical stabilities and outdoor applications [34,35]. The most widely studied inorganic EC material is tungsten trioxide (WO_3). Conventional WO_3-based ECDs are composed of two electrodes, a WO_3 film (cathodic species), a secondary EC film (anodic species), and an electrolyte. Notably, the secondary EC film (or so-called ion storage layer) is essential for low-voltage devices [31-33,40,47]. Soluble anodic species such as ferrocene (Fc) or Fc derivatives has been added directly to the electrolyte to eliminate the need for a secondary film on anode [34,35]. However, most reported WO_3 ECDs have been based on liquid-type electrolytes [28, 29, 34, 35,45-47], which represents a hurdle to the fabrication of flexible/stretchable devices because these electrolytes can leak when films are exposed to mechanical strain.

A few solid electrolytes such as composites of poly(methyl methacrylate) (PMMA, polymer host) and organic solvents (e.g. propylene carbonate (PC) or acetonitrile (ACN)) [31,32,37], and Nafion films containing aqueous sulfuric acid (H_2SO_4) [38] have been developed for WO_3-based ECDs. However, gradual evaporation of high boiling point organic solvents in gel can occur even at room temperature, which may degrade device performance. In addition, electrochemical windows of aqueous electrolytes are too narrow for WO_3 ECDs because of the electrolysis of water. Thus, ion gels consisting of copolymers and room temperature non-volatile ionic liquids, that exhibit rapid ion conduction and high electrochemical stability are considered as promising electrolyte candidates for realizing flexible ECDs based on WO_3 films [48-49].

In this work, we introduced ion gels into WO_3-based ECDs to produce flexible devices. We found that conventional ion gels consisting of poly(vinylidene fluoride-*co*-hexafluoropropylene) (P(VDF-*co*-HFP)) and 1-ethyl-3-methylimidazolium bis(trifluoromethylsulfonyl)imide ([EMI][TFSI]) were not suitable for WO_3 ECDs, because $[EMI]^+$ cations were too large to be inserted into the WO_3 lattice. Therefore, we designed ion gels containing Li^+ ions, for which [Li][TFSI] was employed as a lithium source. The performances of ECDs based on Li-doped ion gels were evaluated in terms of dynamics, coloration efficiency, and optical contrast at various [Li][TFSI] concentrations. The long-term stability of the device with optimized ion gel was also examined. The use of Li-doped gels offers the opportunity to fabricate flexible WO_3 ECDs on plastic. The resulting flexible devices showed good bending stability under various strain ranges. The results imply Li-doped ion gels provide a promising electrolyte platform for flexible, especially WO_3-based, ECDs.

2. Experimental Section

2.1 Materials.

All chemicals except tungsten powder (1-5 microns, 99.9%, Alfa Aesar) were purchased from Sigma-Aldrich and used without additional purification. Tungsten oxide (WO_3) powder was prepared as previously described [34]. WO_3-ink was prepared by mixing WO_3 power, DI water, and isopropyl alcohol at a weight ratio of 0.3:0.35:0.35, and sonicating the resulting mixture to obtain a homogeneous dispersion. Ion gel solution was prepared by blending dimethyl ferrocene(dmFc), poly(vinylidene fluoride-co-hexafluoropropylene) (PVDF-*co*-HFP), 1-ethy-3-methylimidazolium bis(trifluoromethylsulfonyl)imide [EMI][TFSI], and acetone at a weight ratio of 0.44:1:9:20. We added lithium bis(trifluoromethylsulfonyl)imide ([Li][TFSI]) to the EC gel solution as a Li^+ source at [Li][TFSI] to [EMI][TFSI] weight ratios of 0.05, 0.10, to 0.15. Herein, we denoted 0.05 [Li][TFSI] when [Li][TFSI] to [EMI][TFSI] ratio was 0.05. ITO-coated glass (sheet resistance: 15 Ω/sq) was sequentially cleaned with acetone (15 min) and DI-water (15 min) under sonication. However, the ITO-coated PET sheet (sheet resistance: 10 Ω/sq) was used as received.

2.2 Device fabrication and characterization.

The WO_3 dispersion was spin-coated on indium tin oxide(ITO)-coated glass for 20 s at 5000 rpm, and annealed at 60˚C for 6 h in vacuum, which is an optimal condition for the preparation of high performance WO_3 EC layers [35]. The ion gel solution was simply drop-cast on the WO_3 layer. After drying at 60 ^oC, a transparent ion gel was obtained. Another ITO-coated glass was assembled using a double-sided tape to complete device fabrication, in which active WO_3 area was 10 mm × 10 mm. The voltage dependence of absorption spectra, device kinetics, and coloration/bleaching cyclic stability was investigated using a UV-vis spectrometer (UV-1280, Shimadzu), in which applied voltages were supplied by a potentiostat (ZIVE SP1, WonA Tech.). All measurements were performed under ambient conditions.

3. Result and Discussion

In contrast to conventional WO_3-based ECDs, we excluded a secondary anodic film (ion storage layer) by directly incorporating soluble anodic species in the gel (see Scheme 1). Thus, the common gel components were P(VDF-*co*-HFP), [EMI][TFSI], and dimethyl ferrocene (dmFc), which functioned as copolymer, ionic liquid, and anodic species, respectively. After sequential deposition of the WO_3 and ion gel layers on ITO-coated glass, the ion gel layer was covered with another sheet of ITO glass to complete the fabrication. According to the redox reaction of WO_3 (see equation (1)), cations (namely, M^+ in the equation (1)) such as H^+, Li^+ or Na^+ are essential for coloration [22].

$$WO_3(\text{bleached, pale yellow}) + xM^+ + xe^- \rightarrow M_xW^{6+}_{1-x}W^{5+}_xO_3(\text{colored, blue}) \quad (1)$$

Notably acid (e.g. H_2SO_4) is often used to provide H^+ under aqueous conditions [28,38,45,46]. However, aqueous solutions and hydrogels are not suitable for electronics because of the narrow electrochemical window imposed by the presence of water. On the other hand, most common Na^+ ion sources such as sodium chloride (NaCl) are not compatible and cannot be used for ion gels based on [EMI][TFSI] (see Fig. S1 in Electronic Supplementary Information (ESI)). In contrast, [Li][TFSI] is commercially available and fully soluble in [EMI][TFSI]-based gels. Accordingly, the gels were designed to include [Li][TFSI] for successful operation of WO_3 ECDs.

Scheme 1. Schematic illustration of electrochromic devices (ECDs) produced using a WO_3 film and Li-doped ion gel, and molecular structures of components included in the gel.

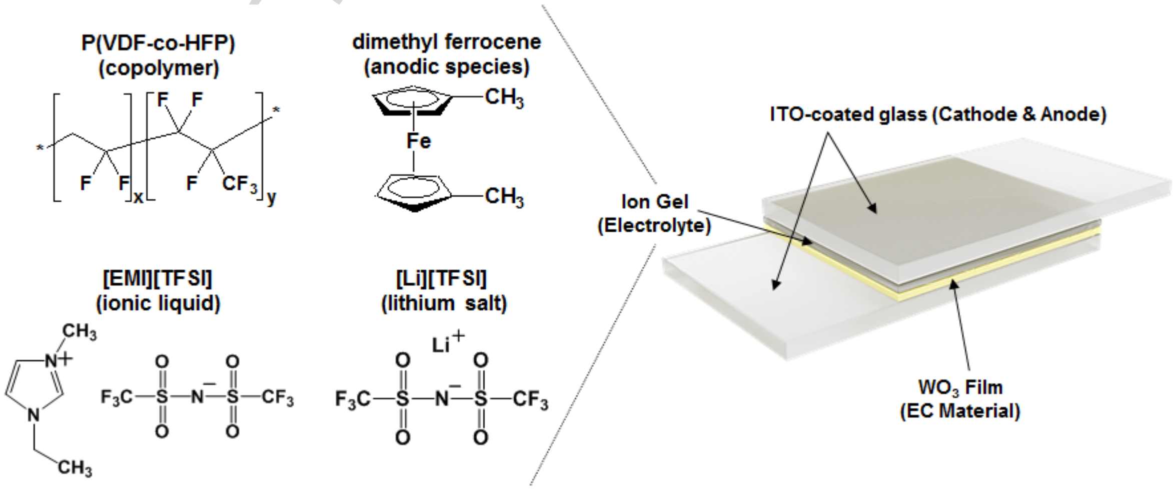

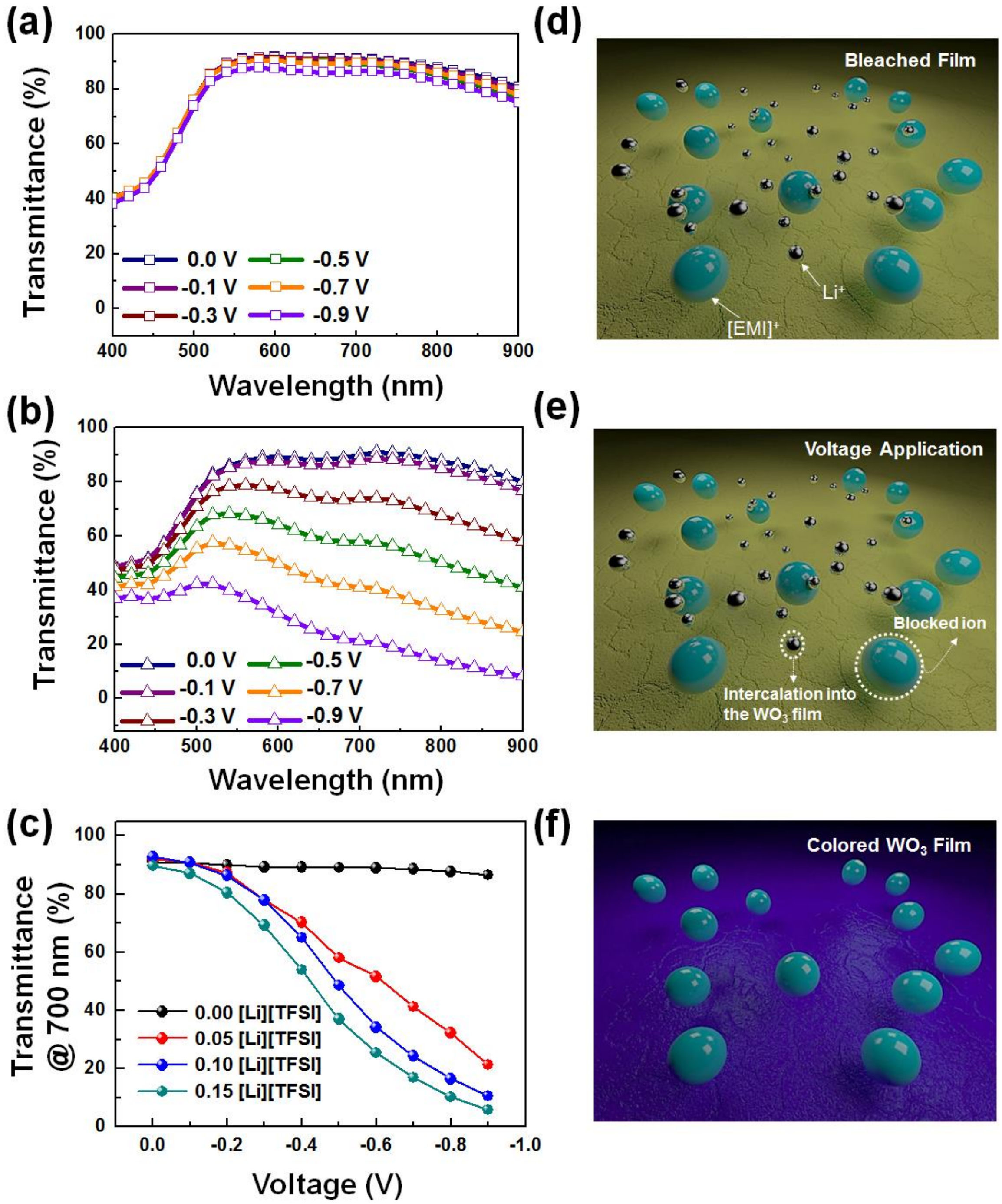

Fig. 1. Voltage dependence of transmittance of ECDs (a) without [Li][TFSI] and (b) with 0.05 [Li][TFSI] in the gel. (c) Plots of transmittance at 700 nm as a function of voltage. (d-f) Schematic illustrations of the coloration mechanism in which large $[EMI]^+$ cations are blocked but relatively small Li^+ ions penetrate the WO_3 layer.

The importance of Li^+ in the gel is demonstrated in Fig. 1. When the ion gel did not contain Li^+ ions, only broad absorption arising from dissolved dmFc was observed (Fig. 1(a)). Furthermore, transmittance spectra did not change even upon application of external voltages, and no coloration was shown. In contrast, dramatic changes in EC behavior were induced by incorporating only 5 wt% [Li][TFSI] with respect to [EMI][TFSI] (Fig. 1(b)). Transmittance in the bleached state was the same as that of the corresponding device without [Li][TFSI], whereas transmittance in the visible range was significantly decreased as voltage was applied. In other words, coloration occurred with the ion gel layer. We also examined the dependence of transmittance at 700 nm on the concentration of [Li][TFSI] (Fig. 1c). Detailed full UV-vis spectra at various voltages for ECDs with 10 and 15wt% [Li][TFSI] were provided in ESI (see Fig. S2 and S3). A larger optical transmittance contrast was detected at a higher [Li][TFSI] content. However, when the [Li][TFSI] content exceeded 10wt% relative to [EMI][TFSI], EC performance approached saturation. Before coloration, $[EMI]^+$ and $[Li]^+$ are present near the WO_3 film (Fig. 1(d)). When voltage is applied, only $[Li]^+$ ions are inserted into the WO_3 film for charge neutrality and coloration occurs (Fig. 1(e) and 1(f)). These results present the importance of Li-doped ion gels for WO_3-based ECDs.

The effect Li^+ concentration on device dynamics was investigated by obtaining transient transmittance profiles. Fig. 2(a) displays the time dependence of transmittance at 700 nm during coloration at different [Li][TFSI] contents. The absence of [Li][TFSI] resulted in no remarkable variation in transmittance (namely, no coloration) even upon application of –0.9 V, which is consistent with Fig. 1(a). As [Li][TFSI] concentration in the gel was increased, the transmittance of the colored state became lower. In other words, the largest transmittance contrast increased from 67.5 % at 0.05 [Li][TFSI] to 84.8 % at 0.15 [Li][TFSI]. Further addition of [Li][TFSI] was not possible due to its limited solubility in the gel. Higher [Li][TFSI] concentrations increased Li^+ diffusion flux into WO_3, so bigger transmittance contrasts and quicker coloration responses were observed (see Fig. 2(a) and Table 1).

On the other hand, more intercalation of Li^+ in the WO_3 layer means that a larger number of Li^+ ions must be extracted to recover the original bleached state, which suggests slower bleaching. Indeed, when we measured bleaching response times (t_b), the longest response time was observed for the device with 0.15 [Li][TFSI] under open- (Fig. 2(b)) and short-circuit conditions (Fig. 2(c)). In particular, the bleaching under short-circuit ($t_{b,short}$ ~ 24 s) was quicker than that under open-circuit condition ($t_{b,open}$ ~ 196 s), which can be explained by differences between bleaching pathways. When the circuit is cut (open-circuit), the chemical reaction between colored WO_3 and $dmFc^+$ diffusion from the counter electrode provides the only means of bleaching. However, an additional bleaching route, direct oxidation of WO_3 near the electrode, becomes available when the circuit is shorted, so the bleahcing is accelerated. This proposal is in good agreement with results obtained using solution electrolyte-based ECDs [34].

We also examined the [Li][TFSI] concentration dependence of coloration efficiency (η) as defined by [22]:

$$\eta = \Delta OD / \Delta Q = \log (T_b / T_c) / \Delta Q \qquad (2)$$

where ΔOD is variation in optical density, T_b and T_c are transmittances in the bleached and colored states, respectively, and ΔQ is the amount of injected charge required to induced ΔOD. From the plots of ΔOD as a function of ΔQ (Fig. 3), η values were estimated by a fit on the linear regime. The extracted η values were 50.1 cm^2/C, 58.2 cm^2/C, and 57.4 cm^2/C for 0.05, 0.10, and 0.15 [Li][TFSI], respectively, which is comparable with the efficiency of optimized solution-based WO_3 ECDs (η ~ 60 cm^2/C) [35].

Table 1. Device characteristics of gel-based WO_3-ECDs as a function of [Li][TFSI] concentration.

[Li][TFSI]/[EMI][TFSI]	ΔT (%)	T_b (%)	T_c (%)	t_c (s)	$t_{b,short}$ (s)	$t_{b,open}$ (s)
0.05	67.5	89.3	21.8	12	12	122
0.10	76.1	88.7	12.6	12.5	20	152
0.15	84.8	89.9	5.1	14	24	196

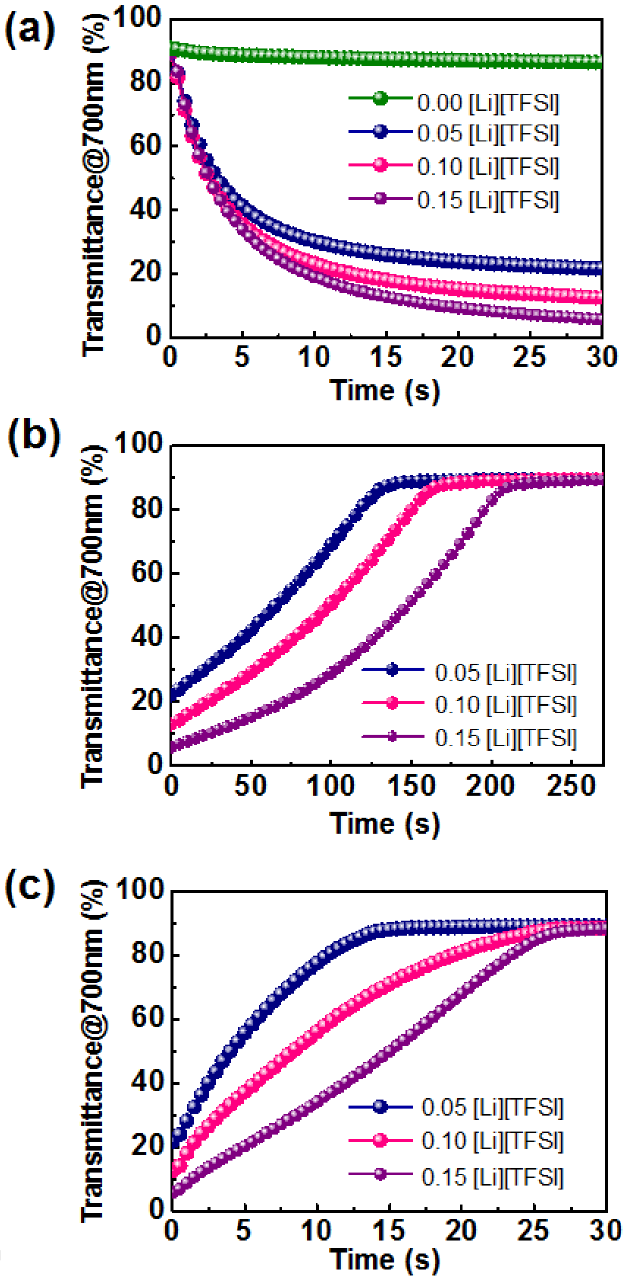

Fig. 2. Transient transmittance profiles at 700 nm for ECDs with various concentrations of [Li][TFSI] during (a) coloration at –0.9 V and bleaching under (b) open- and (c) short-circuit conditions.

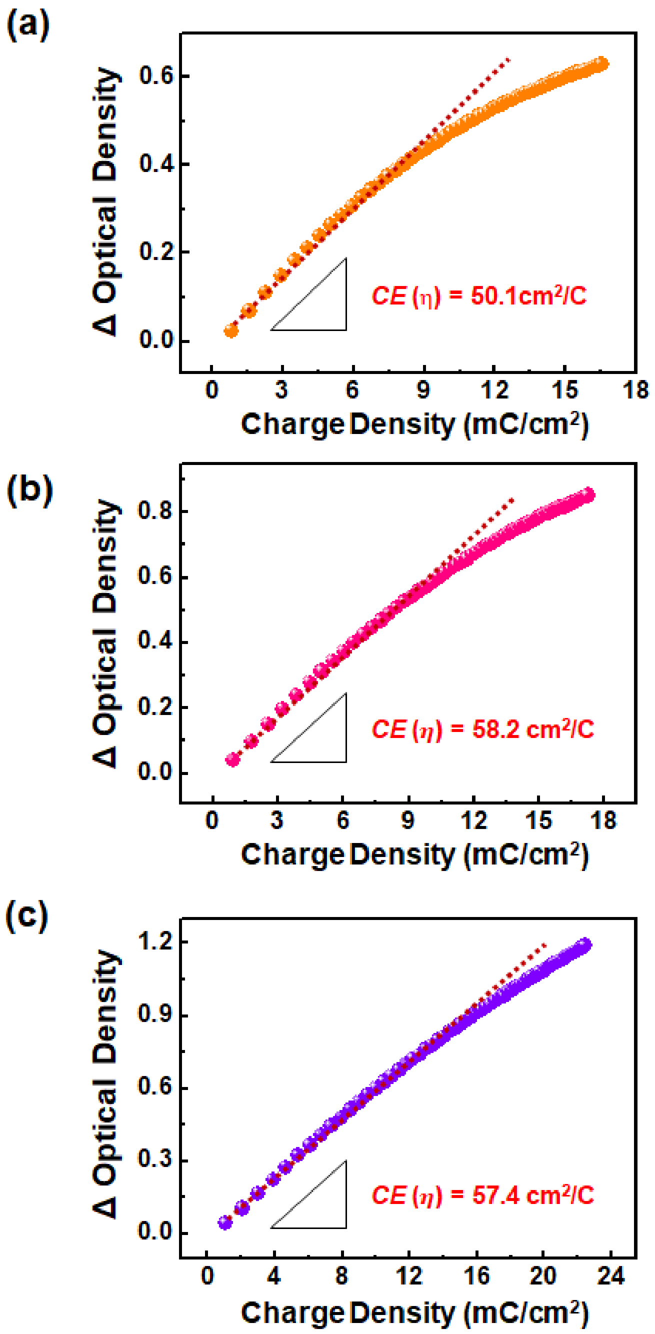

Fig. 3. Charge density dependence of changes in optical density (ΔOD) for ECDs including different [Li][TFSI] concentration in the gel: (a) 0.05, (b) 0.10, and (c) 0.15 [Li][TFSI]. Coloration efficiencies were defined as the slopes of linear fits.

The stable device operation is necessary for practical purpose. Therefore, we tested device stability during repeated coloration and bleaching at 0.10 [Li][TFSI]. As displayed in Fig. 2 and Table 1, coloration response was much faster than bleaching even under short-circuit condition. Accordingly, to recover fully bleached states, we applied an asymmetric square voltage wave (–0.9 V for 5 s (coloration) and 0.0 V for 15 s (bleaching)) during cycle tests. Initially, the transmittance of the device was modulated between ~89% (bleached) and ~35% (colored), and corresponding ΔT was ~54% (see Fig. 4). Even after 24 h continuous operation in air, reversible switching was clearly observed, although a decrease in ΔT was accompanied (*i.e.* T_b ~ 80%, T_c ~ 43%, and thus ΔT ~ 37%).

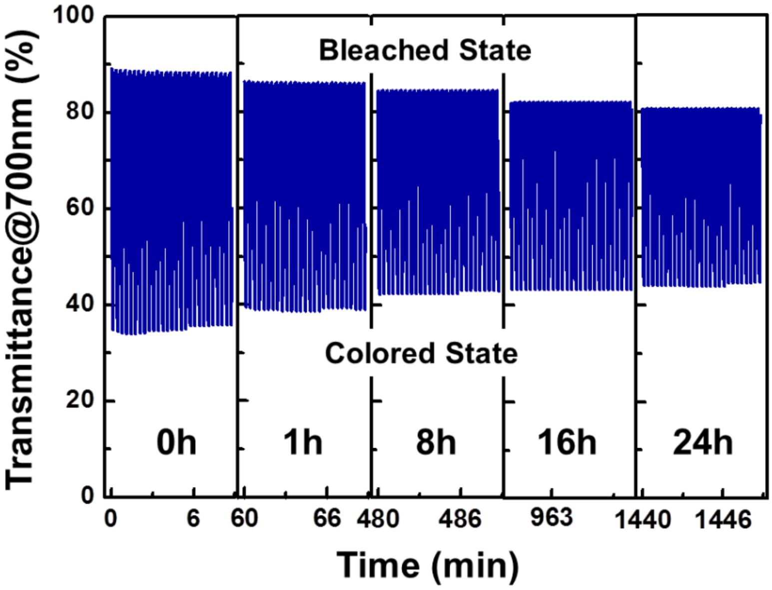

Fig. 4. Operation stability of the ECD at 0.01 [Li][TFSI] during repeated coloration and bleaching cycles. Coloration and bleaching were conducted at –0.9 V and 0.0 V for 5 s and 15 s, respectively.

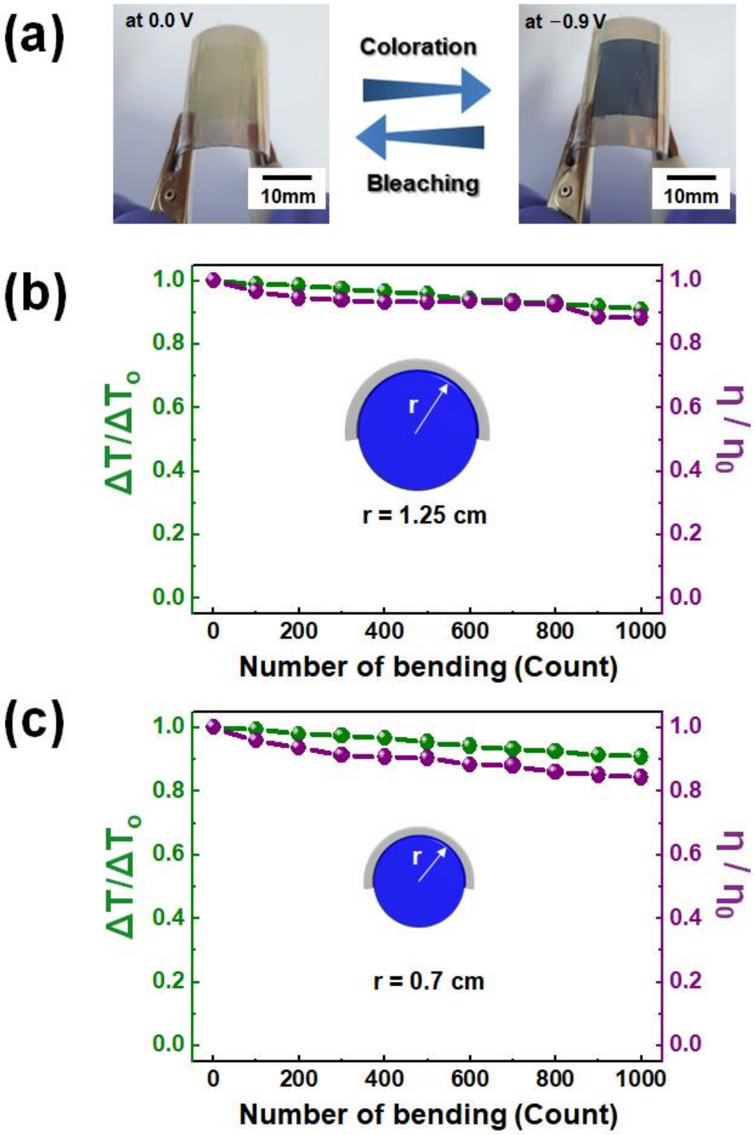

Fig. 5. (a) Photographs of flexible WO_3 ECDs (left: bleached state, right: colored state) with 0.10 [Li][TFSI], in which the size of active area was 10 mm × 10 mm. Bending stability of transmittance contrast (ΔT) and coloration efficiency (η) of the ECD under bending radii of (b) 1.25 cm and (c) 0.7 cm.

The utilizing gel electrolyte layer precludes electrolyte leakage under strain, which offers an opportunity to fabricate flexible devices. Therefore, we fabricated WO_3 ECDs with ITO-coated plastic substrates (*e.g.* ITO-coated polyethylene terephthalate (PET) (Fig. 5(a)), and examined device performances with respect to the number of bending. Two bending radii (R) of 1.25 cm (Fig. 5(b)) and 0.7 cm (Fig. 5(c)) were employed in the test. Corresponding applied strains (ε) were calculated as ~0.5 % and ~0.9%, respectively, based on the equation $\varepsilon = D/2R$ [50] (D is substrate thickness (~125 μm)). The ECDs well-maintained their initial coloration efficiency (η_o) and transmittance contrast (ΔT_o) even after 1000 bendings, although slightly larger decreases in performance were observed under higher strain. One may raise a question if the increase in resistance of ITO-coated plastics due to the damage of ITO layer is the origin of bending instability. Thus, we investigated the resistance of employed ITO-coated PET during bending test. However, a similar level of resistance was maintained (Fig. S4 in the revised ESI), which means there was no issue on the flexible electrode in our experimental conditions. Because the ion gel is elastic, we investigated the reason for the performance degradation of WO_3 films by examining surface morphology after 1000 bendings. As prepared film surfaces were smooth (Fig. S5a). In contrast, when the film was subjected to bending strains, surface cracks were observed. Larger bending deformation can cause more cracks (see Fig. S5b and S5c in ESI) and lead to more performance degradation. It is noted that we did not observe any electrolyte leakage after testing. The EC performances of the devices produced in this work were compared to other gel-based WO_3 ECDs (see Table S1 in ESI). The remarkable features of ECDs containing Li-doped ion gels included (1) good bending stability (ΔT retention ~ 90% after 1000 bends), (2) low operating voltage (–0.9 V), and (3) large transmittance contrast (ΔT ~ 85%) between colored and bleached states. In a previous report [27], we found a gel consisting of 10wt% PVDF-*co*-HFP and 90 wt% [EMI][TFSI] gel simultaneously exhibited good mechanical robustness (storage modulus > 10^4 Pa) and high ionic conductivity (~6.7 mS/cm), which are one of the origins of features (1) and (2), respectively. The dramatic increase in ΔT for ECDs in this work may be due to the absence of a slightly turbid secondary anodic film.

4. Conclusions

In this work, we designed Li-doped ion gels based on consideration of the working principles of WO_3-based ECDs. The ratio between [Li][TFSI] and [EMI][TFSI] was carefully adjusted to optimize device performance. The ECDs at 0.10 [Li][TFSI] exhibited large optical contrast, high efficiency, and cyclic stability. In addition, we successfully demonstrated flexible WO_3-based ECDs that showed good bending stability. The Li-doped ion gels in this work contribute to the fabrication of flexible ECDs based on metal oxides (particularly, WO_3) that do no leak even under bending deformation.

Acknowledgments

This work was supported by the National Research Foundation of Korea (NRF) grant funded by the Korea government (MSIT) (NRF-2016R1C1B2006296), and Human Resources Program in the Transportation Specialized Lighting Core Technology Development (No. N0001364) granted financial resource from the Ministry of Trade, Industry & Energy, Republic of Korea.

References

[1] K. T. Nam, D. -W. Kim, P. J. Yoo, C. -Y. Chiang, N. Meethong, P. T. Hammond, Y. -M. Chiang, A. M. Belcher, Virus-enabled synthesis and assembly of nanowires for lithium ion battery electrodes. Science 312 (2006) 885-888

[2] P. Poizot, S. Laruelle, S. Grugeon, L. Dupont, J. -M. Tarascon, Nano-sized transition-metal oxides as negative-electrode materials for lithium-ion batteries. Nature 407 (2000) 496-499

[3] M. Armand, J. -M. Tarascon, Building better batteries. Nature 451 (2008) 652-657

[4] L. Qie, W. -M. Chen, Z. -H. Wang, Q. -G. Shao, X. Li, L. -X. Yuan, X. -L. Hu, W. -X. Zhang, Y. -H. Huang, Nitrogen-doped porous carbon nanofiber webs as anodes for lithium ion batteries with a superhigh capacity and rate capability. Adv. Mater. 24 (2012) 2047-2050

[5] L. Suo, Y. -S. Hu, H. Li, M. Armand, L. Chen, A new class of solvent-in-salt electrolyte for high-energy rechargeable metallic lithium batteries. Nat. Commun. 4 (2013) 1481-1489

[6] C. Liu, Z. Yu, D. Neff, A. Zhamu, B. Z. Jang, Graphene-based supercapacitor with an ultrahigh energy density. Nano Lett. 10 (2010) 4863-4868

[7] T.-Y. Wei, C. -H. Chen, H. -C. Chien, S. -Y. Lu, C. -C. Hu, A Cost-effective supercapacitor material of ultrahigh specific capacitances: Spinel nickel cobaltite aerogels from an epoxide-driven sol-gel process. Adv. Mater. 22 (2010) 347-351

[8] L. -Q. Mai, F. Yang, Y. -L. Zhao, X. Xu, L. Xu, Y. -Z. Luo, Hierarchical $MnMoO_4/CoMoO_4$ heterostructured nanowires with enhanced supercapacitor performance. Nat. Commun. 2 (2011) 381-385

[9] Q. Wang, Z. H. Wen, J. H. Li, A hybrid supercapacitor fabricated with a carbon nanotube cathode and a TiO_2-B nanowire anode. Adv. Funct. Mater. 16 (2006) 2141-2146

[10] Z. Wen, X. Wang, S. Mao, Z. Bo, H. Kim, S. Cui, G. Lu, X. Feng, J. Chen, Crumpled nitrogen-doped graphene nanosheets with ultrahigh pore volume for high-performance supercapacitor. Adv. Mater. 24 (2012) 5610-5616

[11] X. Dong, Y. Cao, J. Wang, M. B. Chan-Park, L. Wang, W. Huang, P. Chen, Hybrid structure of zinc oxide nanorods and three dimensional graphene foam for supercapacitor and electrochemical sensor applications. RSC Adv. 2 (2012) 4364-4369

[12] X. Kan, H. Zhou, C. Li, A. Zhu, Z. Xing, Z. Zhao, Imprinted electrochemical sensor for dopamine recognition and determination based on a carbon nanotube/polypyrrole film. Electrochim. Acta 63 (2012) 69-75

[13] Z. H. Sheng, X. Q. Zheng, J. Y. Xu, W. J. Bao, F. B. Wang, X. H. Xia, Electrochemical sensor based on nitrogen doped graphene: Simultaneous determination of ascorbic acid, dopamine and uric acid. Biosens. Bioelectron. 34 (2012) 125-131

[14] X. Xie, L. Qu, C. Zhou, Y. Li, J. Zhu, H. Bai, G. Shi, L. Dai, An asymmetrically surface-modified graphene film electrochemical actuator. ACS Nano 4 (2010) 6050-6054

[15] L. Lu, J. Liu, Y. Hu, Y. Zhang, W. Chen, Graphene-stabilized silver nanoparticle electrochemical electrode for actuator design. Adv. Mater. 25 (2013) 1270-1274

[16] J. M. Sansinena, J. Gao, H. L. Wang, High-performance, monolithic polyaniline electrochemical actuators. Adv. Funct. Mater. 13 (2003) 703-709

[17] H. C. Moon, T. P. Lodge, C. D. Frisbie, DC-driven, sub-2 V solid-state electrochemiluminescent devices by incorporating redox coreactants into emissive ion gels. Chem. Mater. 26 (2014) 5358-5364

[18] T. Nobeshima, M. Nakakomi, K. Nakamura, N. Kobayashi, Alternating-current-driven, color-tunable electrochemiluminescent cells. Adv. Optical Mater. 1 (2013) 144-149

[19] H. C. Moon, T. P. Lodge, C. D. Frisbie, Solution-processable electrochemiluminescent ion gels for flexible, low-voltage, emissive displays on plastic. J. Am. Chem. Soc. 136 (2014) 3705-3712

[20] H. C. Moon, T. P. Lodge, C. D. Frisbie, Electrochemiluminescent displays based on ion gels: correlation between device performance and choice of electrolyte. J. Mater. Chem. C 4 (2016) 8448-8453

[21] T. Nobeshima, T. Morimoto, K. Nakamura, N. Kobayashi, Advantage of an AC-driven electrochemiluminescent cell containing a $Ru(bpy)_3^{2+}$ complex for quick response and high efficiency. J. Mater. Chem. 20 (2010) 10630-10633

[22] P. M. S. Monk, R. J. Mortimer, D. R. Rosseinsky, *Electrochromism and Electrochromic Devices*, Cambridge University Press, Cambridge, UK (2007)

[23] D. R. Rosseinsky, R. J. Mortimer, Electrochromic systems and the prospects for devices. Adv. Mater. 13 (2001) 783-793

[24] V. K. Thakur, G. Ding, J. Ma, P. S. Lee, X. Lu, Hybrid materials and polymer electrolytes for electrochromic device applications. Adv. Mater. 24 (2012) 4071-4096

[25] H. C. Moon, T. P. Lodge, C. D. Frisbie, Solution processable, electrochromic ion gels for sub-1 V, flexible displays on plastic. Chem. Mater. 27 (2015) 1420-1425

[26] H. C. Moon, C. -H. Kim, T. P. Lodge, C. D. Frisbie, Multicolored, low-power, flexible electrochromic devices based on ion gels. ACS Appl. Mater. Interfaces 8 (2016) 6252-6260

[27] H. Oh, D. G. Seo, T. Y. Yun, C. Y. Kim, H. C. Moon, Voltage-tunable multicolor, sub-1.5 V, flexible electrochromic devices based on ion gels. ACS Appl. Mater. Interfaces 9 (2017) 7658-7665

[28] M. A. Arvizu, G. A. Niklasson, C. G. Granqvist. Electrochromic $W_{1-x-y}Ti_xMo_yO_3$ thin films made by sputter deposition: Large optical modulation, good cycling durability, and approximate color neutrality. Chem. Mater. 29 (2017) 2246-2253

[29] J. Zhang, J. -P. Tu, X. -H. Xia, X. L. Wang, C. -D. Gu, Hydrothermally synthesized WO_3 nanowire arrays with highly improved electrochromic performance. J. Mater. Chem. 21 (2011) 5492-5498

[30] K. -W. Kim, H. Oh, J. H. Bae, H. Kim, H. C. Moon, S. H. Kim, Electrostatic-force-assisted-dispensing printing of electrochromic gels for low-voltage displays. ACS Appl. Mater. Interfaces 9 (2017) 18994-19000

[31] Q. Liu, G. Dong, Y. Xiao, M. -P. Delplancke-Ogletree, F. Reniers, X. Diao, Electrolytes-relevant cyclic durability of nickel oxide thin films as an ion-storage layer in an all-solid-state complementary electrochromic device. Sol. Energy Mater. Sol. Cells 157 (2016) 844-852

[32] G. Cai, P. Darmawan, M. Cui, J. Chen, X. Wang, A. L. -S. Eh, S. Magdassi, P. S. Lee, Inkjet-printed all solid-state electrochromic devices based on NiO/WO_3 nanoparticle complementary electrode. Nanoscale 8 (2016) 348-357

[33] Zhang, J.; Tu, J. P.; Xia, X. H.; Qiao, Y.; Lu, Y. An All-Solid-State Electrochromic Device Based on NiO/WO_3 Complementary Structure and Solid Hybrid Polyelectrolyte. *Sol. Energy Mater. Sol. Cells.* **2009**, 93, 1840-1845

[34] J. Bae, H. Kim, H. C. Moon, S. H. Kim, Low-voltage, simple WO_3-based electrochromic devices by directly incorporating an anodic species into the electrolyte. J. Mater. Chem. C 4 (2016) 10887-10892

[35] J. Bae, D. G. Seo, S. M. Park, K. T. Park, H. Kim, H. C. Moon, S. H. Kim, Optimized low-temperature fabrication of WO_3 films for electrochromic devices. J. Phys. D: Appl. Phys. 50 (2017) 465105-465112

[36] D. T. Gillaspie, R. C. Tenent, A. C. Dillon, Metal-oxide films for electrochromic applications: present technology and future directions. J. Mater. Chem. 20 (2010) 9585-9592

[37] G. P. T. Ganesh, R. Ravi, B. Deb, A pragmatic approach to methyl methacrylate based solid polymer electrolyte processing: A case study for electrochromism. Sol. Energy Mater. Sol. Cells 140 (2015) 17-24

[38] P. Cossari, A. Cannavale, S. Gambino, G. Gigli, Room temperature processing for solid-state electrochromic devices on single substrate: from glass to flexible plastic. Sol. Energy Mater. Sol. Cells 155 (2016) 411-420

[39] J. Zhou, J. Wang, H. Li, F. Shen, Hybrid gel polymer electrolyte with good stability and its application in electrochromic device. J. Mater. Sci.: Mater. Electronics 29 (2018) 6068-6076

[40] L. N. Sim, F. C. Sentanin, A. Pawlicka, R. Yahya, A. K. Arof, Development of polyarylonitrile-based polymer electrolytes incorporated with lithium bis(trifluoromethane)sulfonimiede for application in electrochromic device. Electrochim. Acta 229 (2017) 22-30

[41] M. Fernandes, R. Leones, A. M. S. Costa, M. M. Silva, S. Pereira, J. F. Mano, E. Fortunato, R. Rego, V. D. Z. Bermudez, Electrochromic devices incorporating biohybrid electrolytes doped with a lithium salt, an ionic liquid or a mixture of both. Electrochim. Acta 161 (2015) 226-235

[42] H. -H. Chou, A. Nguyen, A. Chortos, J. W. F. To, C. Lu, J. Mei, T. Kurosawa, W. -G. Bae, J. B. -H. Tok, Z. Bao, A chameleon-inspired stretchable electronic skin with interactive colour changing controlled by tactile sensing. Nat. Commun. 6 (2015) 8011-8020

[43] P. Chandrasekhar, B. J. Zay, D. Lawrence, E. Caldwell, R. Sheth, R. Stephan, J. Cornwell, Variable-emittance infrared electrochromic skins combining unique conducting polymers, ionic liquid electrolytes, microporous polymer membranes, and semiconductor/polymer coatings, for spacecraft thermal control. J. Appl. Polymer. Sci. 131 (2014) 40850

[44] H. Park, D. S. Kim, S. Y. Hong, C. Kim, J. Y. Yun, S. Y. O, S. W. Jin, Y. R. Jeong, G. T. Kim, J. S. Ha, A skin-integrated transparent and stretchable strain sensor with interactive color-changing electrochromic displays. Nanoscale 9 (2017) 7631-7640

[45] G. Cai, P. Darmawan, M. Cui, J. Wang, J. Chen, S. Magdassi, P. S. Lee, Hyghly stable transparent conductive silver gird/PEDOT:PSS electrodes for integrated bifunctional flexible electrochromic supercapacitors. Adv. Energy Mater. 6 (2016) 1501882

[46] G. Cai, P. Darmawan, X. Cheng, P. S. Lee, Inkjet printed large area multifunctional smart windows. Adv. Energy Mater. 7 (2017) 1602598

[47] Z. Bi, X. Li, Y. Chen, X. He, X. Xu, X. Gao, Large-scale multifunctional electrochromic-energy storage device based on tungsten trioxide monohydrate nanosheets and prussian white. ACS Appl. Mater. Interfaces 9 (2017) 29872-29880

[48] T. P. Lodge, A unique platform for materials design. Science 321 (2008) 50-51

[49] S. Zhang, K. H. Lee, C. D. Frisbie, T. P. Lodge, Ionic conductivity, capacitance, and viscoelastic properties of block copolymer-based ion gels. Macromolecules 44 (2011) 940-949

[50] L. Zhang, H. Wang, Y. Zhao, Y. Guo, W. Hu, G. Yu, Y. Liu, Substrate-free ultra-flexible organic field-effect transistors and five-stage ring oscillators. Adv. Mater. 25 (2013) 5455-5460

Author contribution section

S. H. Kim and H. C. Moon designed the research. T. Y. Yun, X. Li, and J. Bae carried out the experiments. T. Y. Yun, X. Li, S. H. Kim, and H. C. Moon analyzed the experimental data, discussed the results, and wrote the manuscript. T. Y. Yun and X. Li contributed equally to this work.

Graphical abstract

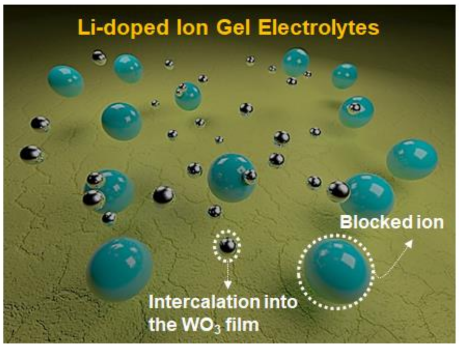

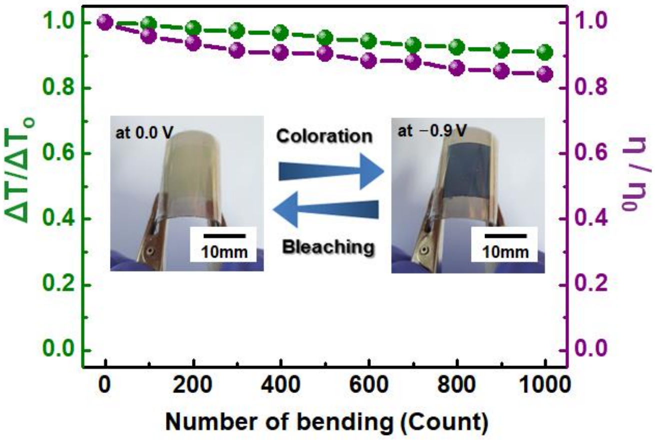

Highlights

- Non-volatile, Li-doped ion gel electrolytes are designed for flexible WO_3-based ECDs.
- ECDs based on Li-doped ion gels exhibit low voltage operation (–0.9 V) and large transmittance contrast (~85%) between colored and bleached states.
- Electrolyte leakage is not observed from flexible ECDs containing Li-doped gel electrolyte when bending deformation is applied.
- Flexible WO_3-based ECDs on plastic maintain ~90.3 and ~84.5% of initial optical transmittance and coloration efficiency, respectively, after 1000 bending tests.